

**Experimental Evaluation of Mixed Fluid Reactions between Supercritical  
Carbon Dioxide and NaCl Brine:  
Relevance to the Integrity of a Geologic Carbon Repository**

John P. Kaszuba<sup>a,\*</sup>, David R. Janecky<sup>b</sup>, and Marjorie G. Snow<sup>c</sup>

Chemical Geology, submitted, 2003

*Isotope and Nuclear Chemistry, Mail Stop J514, Los Alamos National Laboratory, Los Alamos,  
New Mexico 87545 USA*

*<sup>b</sup>Risk Reduction and Environmental Stewardship, Mail Stop J591, Los Alamos National  
Laboratory, Los Alamos, New Mexico 87545 USA*

*<sup>c</sup>Earth and Environmental Sciences, Mail Stop D469, Los Alamos National Laboratory, Los  
Alamos, New Mexico 87545 USA*

\*Corresponding Author: [jkaszuba@lanl.gov](mailto:jkaszuba@lanl.gov), phone (505) 665-7832, FAX (505) 665-4955

LANL LAUR # 03-2978

## ABSTRACT

The reactive behavior of a mixed fluid (supercritical CO<sub>2</sub> and brine) under physical-chemical conditions relevant to geologic storage and sequestration in a carbon repository is largely unknown. Experiments were conducted in a flexible cell hydrothermal apparatus to evaluate fluid-rock (aquifer plus aquitard) reactions that may adversely impact the integrity of the repository. A 5.5 molal NaCl brine-rock system was held at 200°C and 200 bars for 32 days (772 hours) to approach steady state, then injected with CO<sub>2</sub> and allowed to react for an additional 45 days (1079 hours). In a separate experiment at 200°C and 200 bars, the system was allowed to react for 77 days (1845 hours) without injection of CO<sub>2</sub>. Corroded magnesite and euhedral siderite crystallized in a paragenetic sequence after CO<sub>2</sub> injection. Nucleation and growth of siderite on shale suggests the aquitard is a reactive component in the system. Changes in elemental abundances in the brine following addition of CO<sub>2</sub> include pH decrease and depletion of sodium due to accelerated growth of analcime. A pH increase follows pressure and temperature decrease and loss of saturated CO<sub>2</sub> from acidic brine. Silica concentrations and dissolution rates are enhanced and silica precipitation inhibited in the acidic brine.

Geochemical reactions in a carbon repository extend beyond pH decrease and carbonate mineral precipitation. Rock-dominated reaction systems yield to acid-dominated and related reactions controlled by mixed fluid equilibria (*i.e.*, a fluid-dominated system). Silica super-saturation and increased alkalinity associated with mixed fluid phase equilibria could be monitored as geochemical indicators of repository performance. Return of silica super-saturated brine to a rock-dominated reaction system buffered to neutral pH conditions may enhance precipitation of quartz, chalcedony, or amorphous silica. In addition to the potential effects (beneficial or deleterious) that silica super-saturation and precipitation may hold for repository performance, an understanding of the effects of multi-phase equilibrium relationships between supercritical CO<sub>2</sub> and dissolved silica in aquifer-brine systems also raises new questions for a variety of geologic systems. Multi-phase fluid equilibria may, for example, account for quartz cements in some sedimentary basin sandstones and quartz vein mineralization in some ore districts.

**Keywords:** carbon dioxide, geologic sequestration, multi-phase fluids, quartz veins

## 1 INTRODUCTION

A promising approach to the problem of managing anthropogenic carbon is to store and dispose carbon dioxide into geologic formations, including saline aquifers, depleted petroleum reservoirs, and coal deposits. These formations have contained fluids, including natural gas, coal bed methane, and naturally-occurring carbon dioxide, for geologic time and possess a capacity sufficient for disposal of many decades or centuries worth of anthropogenic carbon dioxide (Bachu, 2002). In addition, these formations are widely available and in close proximity to power generation plants (Hitchon *et al.*, 1999), a major source of carbon dioxide emissions.

Geologic formations artificially charged with carbon dioxide are here defined as a *carbon repository*. The carbon repository is a complex structural and stratigraphic package containing diverse geochemical environments, brine and groundwater chemistries, sandstone and shale compositions, lateral facies transitions, *etc.* Overlying confining beds (aquitards) must also be considered as a part of this potentially rich reaction environment, the stability of which are critical to long-term containment of carbon dioxide. The environment of a carbon repository would also span a range of depths for initial emplacement and subsequent migration, and therefore a range of pressures and temperatures of geochemical interest. Pressures may range from a few bars where carbon dioxide has migrated to the near-surface to several hundreds of bars within the initial zone of emplacement. Temperatures may range as high as 150-200°C, depending on local and regional geothermal gradients. Within this environment, carbon dioxide will be in the supercritical state, because its critical point lies at approximately 31°C and 74 bars (Span and Wagner, 1996), and will be immiscible in water (Takenouchi and Kennedy, 1964).

Emplacement of carbon dioxide into a carbon repository and the mechanisms for retention therein are discussed in detail elsewhere (Bachu *et al.*, 1994). Broadly speaking, mineral precipitation can be referred to as sequestration whereas stratigraphic and/or structural trapping and hydrodynamic trapping can be termed storage. Sequestration, therefore, implies the tying up of carbon in a geologically-stable form whereas storage implies a potentially shorter-term method.

Far less attention has been paid to mechanisms that adversely impact the integrity of a carbon repository. Lindeberg (1997) was among the first to quantitatively evaluate escape mechanisms of carbon dioxide emplaced in a saline aquifer. With simple

numerical models incorporating the Darcy equation and Fick's law, Lindeberg (1997) attributed leakage of carbon dioxide to gravity migration with subsequent release through subvertical fractures and faults. More recently, numeric simulations were used to evaluate injection of carbon dioxide into a brine aquifer and calculate the potential for leakage by discharge along a fracture or fault zone (Ennis-King and Paterson, 2000; Pruess and Garcia, 2002; Saripalli and McGrail, 2002) and by caprock failure (Rutqvist and Tsang, 2002). These simulations did not evaluate the effects of geochemical reactions (positive or negative) on injection and leakage of carbon dioxide.

A few experimental studies do examine geochemical reactions in a saline aquifer in response to injection of carbon dioxide under repository conditions. In numerical geochemical modeling studies that incorporate kinetic rate laws (Gunter *et al.*, 2000; Perkins and Gunter, 1995) and one study combining experiment and modeling (Gunter *et al.*, 1997), dissolution of silicate minerals in a brine and precipitation of carbonate are reported. In their investigation, Kaszuba *et al.* (2003) identified geochemical reactions within an experimental system at reservoir temperature and pressure and began to identify potential failure modes due to geochemical mechanisms.

The purpose of this study is to evaluate an experimental brine-rock (aquifer plus aquitard) system that simulates a carbon repository for fluid-rock reactions that may adversely impact the integrity of the repository. Geochemical behavior of multiphase and supercritical  $\text{CO}_2$  fluid in this system will defy simplistic field sampling, assumptions and predictions because the reactions will involve a two-phase fluid (supercritical carbon dioxide and brine). Therefore, evidence for fluid-rock reactions that may be detrimental to the repository include experimental data, natural reaction textures on minerals comprising the aquitard, and deleterious changes in brine chemistry. A carbon repository will exhibit a wide range of temperature and pressure, approximately 50-200°C and 20-1000 bars (Bachu, 2000; Benson, 2000; Carter *et al.*, 1998; Hitchon *et al.*, 1999; Hurter and Pollack, 1996; Oldenburg *et al.*, 2001). The relatively high temperature of 200°C was selected for this study for consistency with the experimental work of Kaszuba *et al.* (2003) and so that kinetic rates of silicate reactions would be maximized. A pressure of 200 bars was chosen for consistency with Kaszuba *et al.* (2003) and accessibility for sequestration scenarios. NaCl brine without significant impurity was used as the initial fluid to emphasize reactions in the rock.

Evidence for reactions involving the aquitard and potentially deleterious changes in brine chemistry were observed in our experiments, from which a number of clear implications can be drawn regarding the integrity of a carbon repository. The discussion is also extended to other geochemical systems in which supercritical carbon dioxide may have impact.

## 2 MATERIAL AND METHODS

### 2.1 Experimental Approach

A model aquifer-aquitard geochemical system was reacted with brine at 200°C and 200 bars for 32 days (772 hours) to approach steady state. Carbon dioxide was then injected into the system and the experiment continued for another 45 days (1079 hours). At 200°C and 200 bars, carbon dioxide in the reaction cell is a supercritical fluid that is largely immiscible, but not totally insoluble, in brine (Figure 1) and free to react with the aquifer-aquitard-brine system. To provide a basis of understanding for the effect of the two fluids in this experiment, a separate brine-rock experiment was allowed to react for 77 days (1845 hours) at 200°C and 200 bars and without injection of carbon dioxide. Brine was periodically sampled and analyzed during both experiments. After the experiments were terminated, the solids and quenched brine were analyzed.

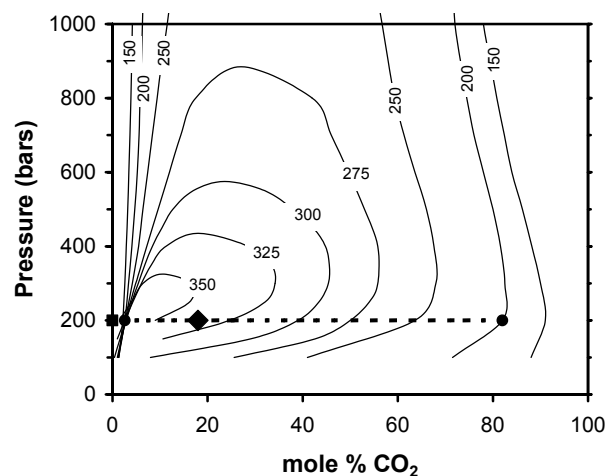


Figure 1. Pressure- $X_{\text{CO}_2}$  phase diagram for  $\text{H}_2\text{O} + \text{CO}_2$  with consolute curves for temperatures of 150 to 350°C (after Takenouchi and Kennedy, 1964). Bulk compositions of the experimental reactions for brine-rock (square) and supercritical  $\text{CO}_2$ -brine-rock after injection of  $\text{CO}_2$  (diamond) are also plotted. The dashed line represents the phase relationships specific to the supercritical  $\text{CO}_2$ -brine-rock experiment at 200°C and 200 bars.

## 2.2 Experimental Apparatus

The experiment was conducted in a flexible cell hydrothermal apparatus consisting of a gold-titanium reaction cell contained within a steel pressure vessel (Seyfried *et al.*, 1987). The cell is plumbed to a valved capillary tube that serves as a sampling port. This equipment allows fluid samples to be withdrawn from the gold reaction cell at the temperature and pressure of an experiment and to be rapidly cooled to ambient conditions in less than a few seconds. Consequently, retrograde reactions with minerals that may occur during a prolonged quench process are avoided and solution composition can be analyzed along a reaction pathway. Fluids such as carbon dioxide can also be introduced into the reaction cell during an experiment to allow external modification of the fluid composition (Kaszuba *et al.*, 2003). This equipment also allows external control and monitoring of pressure and temperature.

## 2.3 Materials

Arkose was chosen as the geochemical and mineralogical representation of an aquifer for these experiments because it provides a diverse geochemical reaction basis and commonly occurs as the reservoir host in sedimentary basins. The arkose was constructed from equal amounts of naturally-occurring Minas Gerais quartz, oligoclase ( $An_{17-21}$ ), and microcline ( $Or_{91-97}$ ) exhibiting perthitic exsolution ( $Or_{3-9}$ ) as described in Kaszuba *et al.* (2003). Biotite was also added as a proxy for ferromagnesian minerals that occur in arkoses. A sample from the Silurian Maplewood Shale, an argillaceous shale from Monroe County, New York, USA, was selected as a geochemical representation of an aquitard, as described in Kaszuba *et al.* (2003).

NaCl brine (Tables 1 and 2) was modeled after saline aquifer compositions and synthesized using standard laboratory-grade salt. The ionic strength of the brine is 5.5 molal.

The supercritical carbon dioxide-brine-rock experiment was performed in a gold reaction cell loaded with 3.1 grams of arkose (1:1:1:0.3 quartz:plagioclase:microcline:biotite), 2.7 grams of Maplewood Shale chips, and 90 grams of brine. Following extraction of 33.3 grams of brine as samples during the initial 771 hours of reactions, approximately 6 grams of carbon dioxide was injected into the reaction cell. Thus, the initial brine to rock mass ratio was 15.5:1 and the initial brine to carbon dioxide mass ratio was approximately 9.5:1. The brine-rock experiment was performed in a smaller titanium reaction cell loaded with 2.2 grams of arkose (1:1:1:0.3 quartz:plagioclase:microcline:biotite), 1.9 grams of Maplewood Shale chips, and 64.1 grams of brine.

The initial brine to rock mass ratio for this experiment was also 15.5:1.

## 2.4 Analytical Methods

Hydrothermal fluids within the reaction cell were sampled as described by Seyfried *et al.* (1987). Dissolved Si, Ca, Mg, Na, K, and B were determined by ICP-ES, dissolved Al, Fe, and Mn by ICP-MS, and dissolved anions by ion chromatography. Total carbon as carbon dioxide was determined by coulometric titration (Huffmann, 1977). Analytical precision of analyses is reported in Tables 1 and 2. Solids were analyzed using optical microscopy and scanning electron microscopy (SEM). Secondary and backscattered electron signals and qualitative X-Ray analysis using Energy Dispersive Spectrometry (EDS) were used in SEM analysis.

# 3 EXPERIMENTAL RESULTS

## 3.1 Brine Chemistry during Reactions

Initial fluctuations observed in brine chemistries, as recorded in the first fluid samples collected at approximately 340 hours (Tables 1 and 2), reflect adjustment of brine to rock. Concentrations of Na and Cl in the brines decrease by approximately 15% (Figure 2). Initial pH (measured as 8 at 25°C and calculated as 6.6 at 200°C, Figure 3) decreased by approximately 1.5 units (2 units in the sample measured at 25°C). Trace ions previously absent from NaCl brine appeared in solution at millimolar (K, Ca, and  $SiO_2$ ) to micromolar (Mg, Al, Fe and Mn) quantities (Figures 4 and 5).

In the brine-rock experiment, the initial decrease of the Na concentration is followed by a 2.5% increase at 671 hours (Table 1, Figure 2). The Na concentration subsequently decreases for the duration of the experiment. Although this decrease falls within the analytical uncertainty, our interpretation of Na decrease is consistent with the precipitation of analcime as discussed in the next section. At the rate of decrease observed in the final 800 hours of the experiment, an additional 1000 hours would be needed to determine the Na decrease beyond the limits of uncertainty. The initial Cl decrease is followed by a 2% decrease at 671 hours and a 7% increase at 1007 hours. These changes, however, are within the 5% uncertainty of Cl analyses. After 1007 hours, the Cl concentration remained stable for the duration of the experiment. After the initial pH decrease, the *in-situ* pH of approximately 5 (measured pH of approximately 5.9) remained stable for the duration of the experiment (Figure 3). The stabilization of Na and Cl concentrations and pH suggests that the brine achieved an approximate

Table 1. Water chemistry (millimole/Kg), brine-rock experiment, 200°C, 200 bars.

Time (hours)	pH	Na	<sup>a</sup> K	<sup>a</sup> Ca	<sup>a</sup> Mg	Cl	Br	SO <sub>4</sub>	<sup>a</sup> SiO <sub>2</sub>	<sup>a</sup> Al	Fe	Mn	<sup>a</sup> B
Initial Brine	8.00	4852	0.19	0.07	0.009	4865	<0.06	<0.1	0.06	0.005	<0.002	<0.0004	0.19
335	5.92	4135	2.38	2.84	0.074	4183	<0.06	<0.1	2.46	0.015	0.061	0.012	0.07
671	5.91	4239	2.63	2.99	0.047	4099	<0.06	<0.1	2.49	0.007	0.005	0.013	0.21
1007	5.86	4257	3.45	3.27	0.057	4397	<0.06	0.09	2.48	<0.004	0.004	0.014	0.27
1841	5.80	4200	3.99	3.67	0.062	4411	<0.06	0.09	2.57	<0.004	0.008	0.019	0.21
Quench													
1845	5.95	4148	3.94	3.67	0.074	4294	<0.06	0.09	2.42	<0.004	0.010	0.020	0.17
<sup>c</sup> maximum 2σ uncertainty	4%	1%	6%	1%	<sup>b</sup> 1%	5%	5%	5%	1%	<sup>b</sup> 12%	2%	<sup>b</sup> 2%	<sup>b</sup> 1%

<sup>a</sup>Laboratory-grade NaCl salt was used to synthesize the brine. Low concentrations of ions other than Na or Cl measured in the initial brine are from impurities in the NaCl salt (*e.g.* K and B).

<sup>b</sup>Higher analytical uncertainty for trace constituents in initial brine (4% for Mg, 20% for Al, 3% for B) and for sample at 1007 hours (4% for Mg and 5% for Mn).

<sup>c</sup>Excluding pH, charge balance is within 96% for all analyses except initial brine and sample at 671 hours, which balance to within 99%.

Table 2. Water chemistry (millimole/Kg), supercritical carbon dioxide-brine-rock experiment, 200°C, 200 bars.

Time (hours)	pH	Na	K	Ca	Mg	Cl	Br	SO <sub>4</sub>	SiO <sub>2</sub>	Al	Fe	Mn	B	ΣCO <sub>2</sub>
Initial Brine	8.00	4851	<0.13	0.02	0.02	5098	<0.06	<0.1	<0.04	<0.04	<0.01	<0.002	0.03	0.09
339	6.07	4339	2.51	2.64	0.25	4253	<0.06	0.4	2.10	<0.04	0.045	0.011	0.10	---
771	5.83	4112	2.56	3.42	0.45	4233	<0.06	<0.1	2.91	<0.04	0.011	0.013	0.35	5.2
Inject CO <sub>2</sub>														
772	---	---	---	---	---	---	---	---	---	---	---	---	---	---
842	6.57	4007	2.52	3.94	3.47	4142	<0.06	<0.1	5.34	<0.04	0.94	0.067	0.40	269
1011	6.68	3886	2.61	3.87	4.05	4145	<0.06	<0.1	5.52	<0.04	1.22	0.057	0.26	301
1179	6.46	3984	2.81	3.74	3.98	3899	<0.06	<0.1	5.55	<0.04	1.02	0.055	0.18	240
1850	6.62	3600	2.97	4.12	3.88	4006	<0.06	0.2	7.72	<0.04	0.885	0.054	0.30	271
Quench														
1851	---	3639	2.99	4.12	4.12	3924	<0.06	0.2	6.73	<0.04	0.577	0.058	0.14	---
<sup>a</sup> maximum 2σ uncertainty	4%	2%	7%	1%	2%	5%	5%	5%	3%	NA	2%	5%	7%	10%

<sup>a</sup>Analytical uncertainty in analysis of the initial brine is 7% for Ca, 42% for Mg, and 30% for B. Excluding pH, charge balances within 95% for all analyses except final sample (1850 hours and quench sample), which balance within 90%.

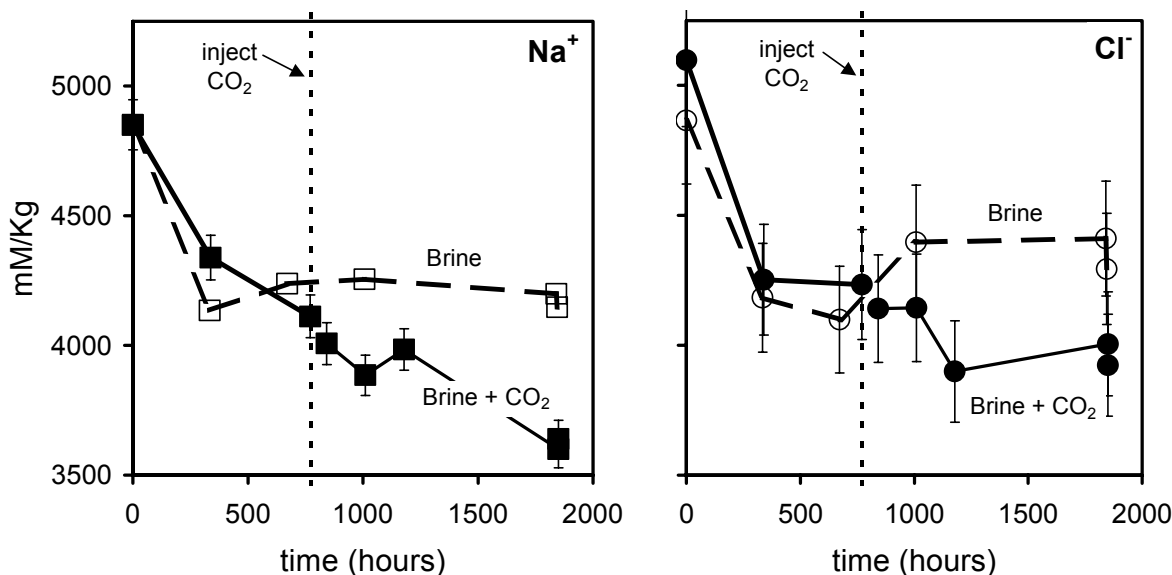


Figure 3. Brine chemistry as a function of time for sodium (figure at left) and chloride (figure at right) during the experimental reaction for brine-rock (open symbols and dashed lines) and supercritical CO<sub>2</sub>-brine-rock (solid symbols and lines). The initial brine to rock mass ratio in both experiments was 15.5:1. Carbon dioxide was injected into the reaction cell of the supercritical CO<sub>2</sub>-brine-rock experiment (6 g CO<sub>2</sub> into 56.7 g brine) at 772 hours (vertical dashed line) to produce a fluid to rock ratio of ~10/1/1 for brine/CO<sub>2</sub>/rock. A two-phase fluid (brine + supercritical CO<sub>2</sub>) was also formed. Uncertainties for sodium in the brine-rock experiment are smaller than the size of the symbols. Error bars represent uncertainties for sodium in the supercritical CO<sub>2</sub>-brine-rock experiment and for chloride. Samples collected after each experiment was terminated are represented by the last symbol shown for each analyte.

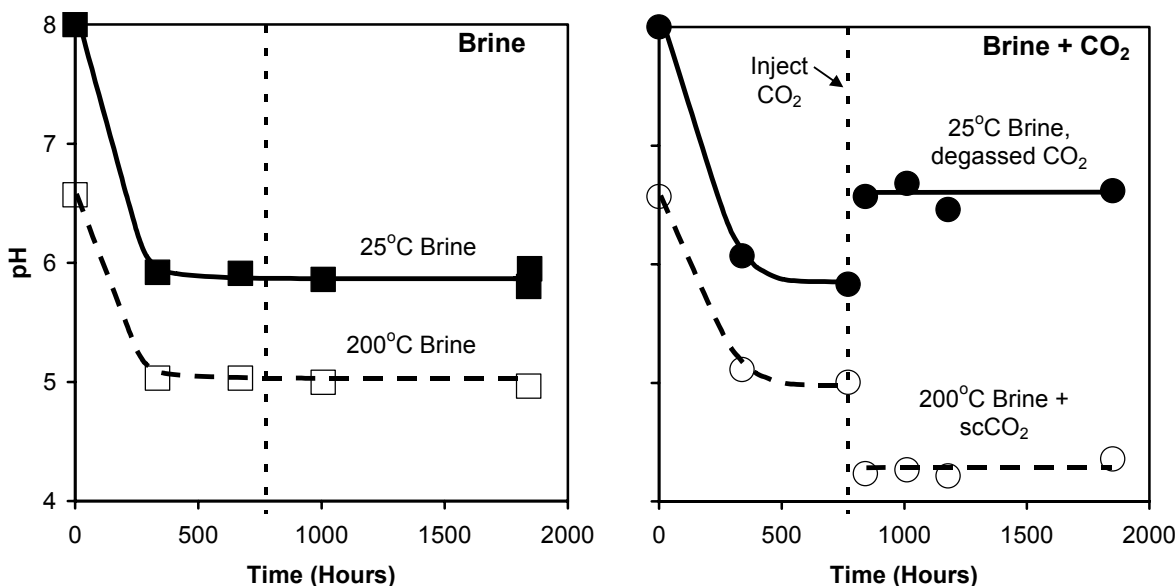


Figure 2. Interpretation of pH behavior during the experimental reaction for brine-rock (figure at left) and supercritical CO<sub>2</sub>-brine-rock (figure at right). For both experiments, pH is measured at 25°C, 1 bar in samples from which CO<sub>2</sub> has degassed (solid lines and symbols). Calculation of pH using Geochemist's Workbench and the b-dot ion association model (Bethke, 1998) for brine samples at 200°C indicates an *in-situ* pH (dashed lines and open symbols). In both experiments, *in-situ* pH decreases from 6.6 to approximately 5 by the time the first sample is collected. Following injection of CO<sub>2</sub> into the supercritical CO<sub>2</sub>-brine-rock experiment, *in-situ* pH further decreases to approximately 4.2 (open circles). At 25°C, pH measured in degassed brine from this experiment is approximately 6.6 (solid circles). Uncertainties are equal to the size of the symbols.

steady state with respect to the major elements and pH, controlled by the alteration mineral assemblage.

In contrast to Na, Cl, and pH, the concentrations of trace elements did not stabilize in the latter stages of the brine-rock experiment (Tables 1 and 2, Figures 4 and 5). Because these ions are present in trace amounts, they may be indicators of more subtle changes in the alteration mineral assemblage. After the 335-hour sample, the SiO<sub>2</sub> concentration was stable to 1007 hours, then increased by approximately 4% in the final sample (1841 hours). These SiO<sub>2</sub> concentrations are below the calculated solubility of quartz. The Mg concentration decreased between 335 and 671 hours, then increased throughout the duration of the experiment, although the apparent rate of increase diminishes in the latter portion of the experiment. The Mn concentration increased throughout the duration of the experiment, and the apparent rate of increase was greatest between the last two samples collected. The Fe concentration decreased between 335 and 1007 hours, after which it increased. The Ca and K concentrations increased throughout the duration of the experiment.

In the time preceding injection of CO<sub>2</sub> into the supercritical CO<sub>2</sub>-brine-rock experiment (the first 771 hours), pH and concentrations of Na, Cl, and trace elements were similar to concentrations in the initial 770 hours of the brine-rock experiment (Tables 1 and 2, Figures 2-5). The exception is Mg, with concentrations 3 to 10 times larger than observed in the brine-rock experiment. The reason for this difference is unknown. However, at least some of the differences between chemical analyses from these two experiments can be attributed to the difficulties of obtaining reliable chemical analyses in brine, as indicated by the 4-5% charge imbalance in analyses and the 5% uncertainty in anion analyses.

Injection of approximately 6 grams of CO<sub>2</sub> into the reaction cell of the supercritical CO<sub>2</sub>-brine-rock experiment at 772 hours increased the pressure of the experimental system from 196 to 254 bars. The pressure decreased by a total of 24 bars over the following 39 hours. The system pressure subsequently stabilized at approximately 230 bars for the duration of the experiment, with fluctuations of a few bars that were correlated to ambient temperature changes in the laboratory and experimental apparatus. The 24 bar pressure decrease is consistent with previously observed behavior (Kaszuba and Janecky, 2000; Kaszuba *et al.*, 2003).

Injection of CO<sub>2</sub> into the supercritical CO<sub>2</sub>-brine-rock experiment also produced significant changes in the brine, changes that are apparent by comparing the brine chemistry between the two experiments. Na and Cl concentrations and pH decreased, as measured

in the sampling event held 70 hours after injection of CO<sub>2</sub> (Tables 1 and 2, Figures 2 and 3). The concentration of Na continued to decrease and did not stabilize. The concentration of Na in the sample collected immediately prior to termination of the experiment was approximately 12% less than the Na concentration of the sample collected 1 hour before injection of CO<sub>2</sub> and 14% less than the Na concentration of the brine-rock experiment. The concentration of Cl decreased by approximately 8% until 1179 hours (407 hours after CO<sub>2</sub> injection), then stabilized at a concentration approximately 11% less than that of the brine-rock experiment. The apparent late increase in Cl concentration (compare data between 1179 and 1850 hours) is within the 5% uncertainty for anion analyses (Table 2). The *in-situ* pH abruptly decreased to approximately 4.2, a pH that is 0.8 units lower than observed in the brine-rock experiment, and stabilized for the duration of this experiment. At 25°C, the pH measured in degassed brine from this experiment rebounded to approximately 6.6. This pH is approximately 0.8 units higher than the pH measured in brine samples from the final 1000 hours of the brine-experiment.

In contrast to changes in Na and Cl concentrations and pH, most trace element concentrations abruptly increased (Ca, 15%; Mg, 8x; SiO<sub>2</sub>, 80%; Fe, 100x; and Mn, 5x) in the first sample collected (842 hours) after CO<sub>2</sub> was injected (Tables 1 and 2, Figures 4 and 5). The K concentration exhibited no measurable change in this same interval. The Ca concentration decreased by 5% from 842 to 1179 hours, then increased by 10% for the duration of the experiment. Ca concentrations increased in the latter stages of both experiments but are 12 to 18% higher in the supercritical CO<sub>2</sub>-brine-rock experiment. Concentrations of Mg and Fe increased by 15 and 30%, respectively, from 842 to 1011 hours, then decreased by approximately 4% to 30% for the duration of the experiment. In contrast to the brine-rock experiment, the Mg and Fe concentrations were approximately an order of magnitude greater and decreased in the latter stages of the experiment. The SiO<sub>2</sub> concentration increased by 3% from 842 to 1011 hours (70 to 239 hours after injecting CO<sub>2</sub>). It remained stable until 1179 hours (407 hours after injecting CO<sub>2</sub>) at a concentration approximately twice that of the brine-rock experiment, then increased by 40% for the duration of the experiment. The rate of increase of SiO<sub>2</sub> concentration is approximately 30 times greater compared to the brine-rock experiment. Unlike the brine-rock experiment, SiO<sub>2</sub> concentrations are greater than the calculated solubility of quartz. The Mn concentration decreased by a total of 20% whereas the K concentration increased by a total of 18% between 842 hours and

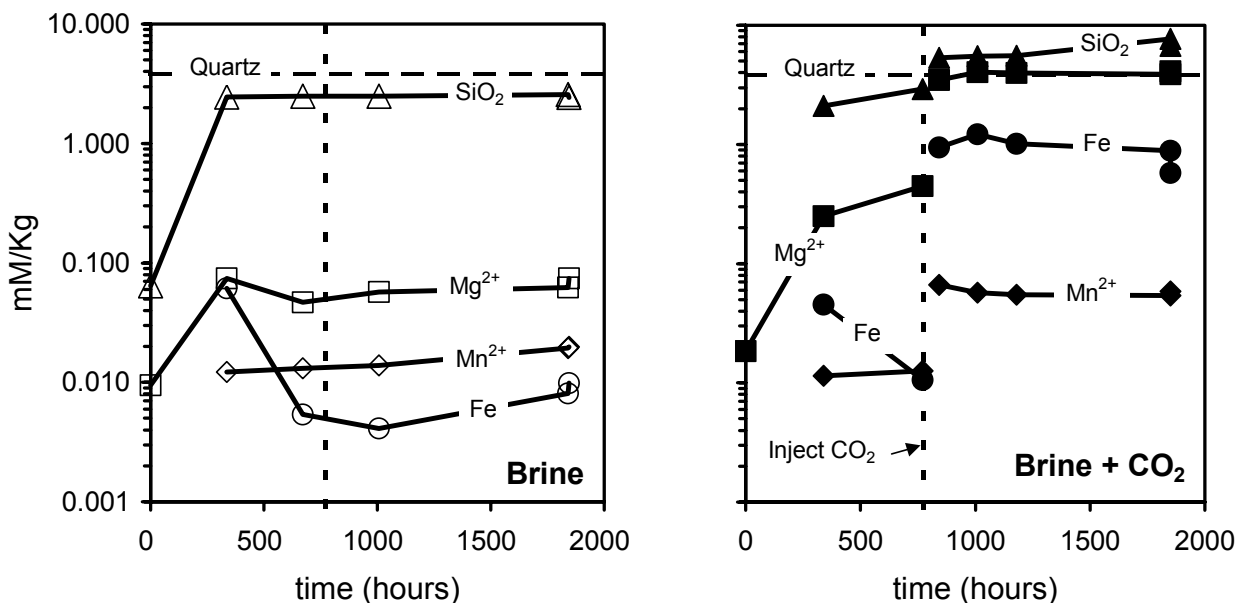


Figure 4. Brine chemistry as a function of time for SiO<sub>2</sub> (triangles), Mg (squares), Mn (diamonds), and Fe (circles) during experimental reaction of brine-rock (figure at left) and supercritical CO<sub>2</sub>-brine-rock (figure at right). The vertical dashed line at 772 hours indicates injection of carbon dioxide into the reaction cell of the supercritical CO<sub>2</sub>-brine-rock experiment (figure on right). The vertical dashed line is repeated in the figure on the left (brine-rock experiment) for reference. Horizontal dashed line is calculated quartz solubility. Uncertainties are smaller than the size of the symbols. Samples collected after each experiment was terminated are represented by the last symbol shown for each analyte.

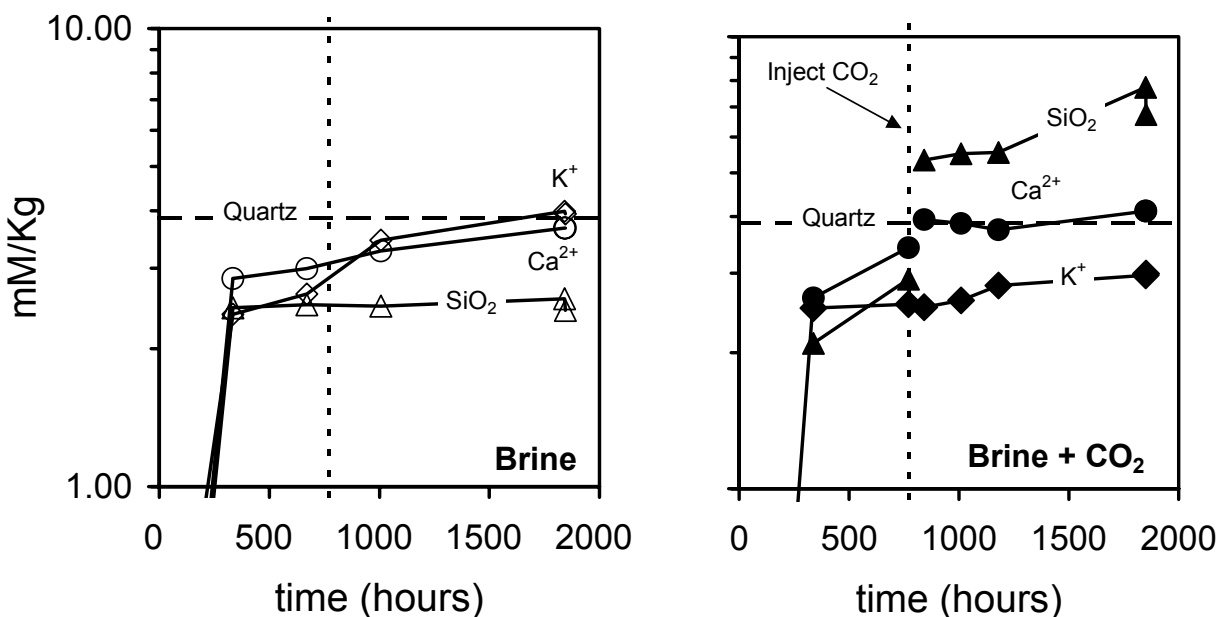


Figure 5. Brine chemistry as a function of time for Ca (circles) and K (diamonds) during experimental reaction of brine-rock (figure at left) and supercritical CO<sub>2</sub>-brine-rock (figure at right). Calculated quartz solubility (horizontal dashed line) and SiO<sub>2</sub> (triangles) from Figure 3 are plotted for reference. Uncertainties are smaller than the size of the symbols. Ca and K in samples collected after each experiment was terminated are nearly identical to the last sample collected at pressure and temperature.



the termination of the experiment. The Mn concentrations were approximately 5 times greater and decreased throughout the latter stages of this experiment as compared to the brine-rock experiment. While the K concentrations increased in both experiments, they are approximately 30% less in this experiment. K is the only trace element in this experiment that is present in smaller amounts than in the brine-rock experiment. The significant increase in concentration of most trace elements suggests the rock dissolved by reaction with CO<sub>2</sub> and brine, behavior consistent with the *in-situ* pH decrease and increased CO<sub>2</sub> dissolved in brine due to carbon dioxide injection. The pressure drop observed in the reaction system, therefore, appears to be an external measure of the overall supercritical CO<sub>2</sub>-brine-rock reaction rate for this process.

Concentrations of several of the ions in brine samples collected after the experiment were terminated were different from concentrations in samples collected immediately prior to termination. In the brine-rock experiment, the SiO<sub>2</sub> concentrations were smaller by 6% whereas Mg (19%), Fe (25%), and Mn (5%) concentrations were greater. In the supercritical CO<sub>2</sub>-brine-rock experiment, SiO<sub>2</sub> (13%) and Fe (35%) concentrations were smaller whereas Mg (6%) and Mn (7%) concentrations were greater. Na, K, Ca, and Cl concentrations exhibited no change in either experiment.

### 3.2 Reaction of Solid Phases

While carbonate minerals did not precipitate in the brine-rock experiment, two types of carbonate minerals precipitated in the supercritical carbon dioxide-brine-rock experiment. Magnesite occurs as large (up to several mm in length), discrete, bladed crystals visible to the naked eye (Figure 6). The crystal faces of the magnesite are pitted and rough, suggesting that magnesite was not in equilibrium with the mixed fluid phase at the time the experiment was terminated. Siderite occurs as euhedral crystals, about 200-250  $\mu\text{m}$  in diameter, on the shale (Figure 7). The euhedral texture suggests that siderite was an equilibrium phase at the time the experiment was terminated. Qualitative X-ray analysis using EDS confirmed the identification of both minerals, and neither was present in the mineral assemblage at the beginning of this experiment. Therefore, we interpret the carbonate mineral assemblage as precipitation of magnesite after injection of carbon dioxide, followed by magnesite dissolution and siderite precipitation.

Analcime trapezohedrons are ubiquitous to both experiments (Figures 7 and 8) as euhedral crystals, 20-40  $\mu\text{m}$  in diameter, occurring on the shale as well as the minerals comprising the aquifer. Euhedral analcime is more abundant in the brine-rock experiment as compared to the supercritical CO<sub>2</sub>-brine-rock experiment. Euhedral textures suggest that analcime crystallized as an equilibrium phase in both experiments. Analcime also occurs as masses of skeletal crystals in the supercritical CO<sub>2</sub>-brine-rock

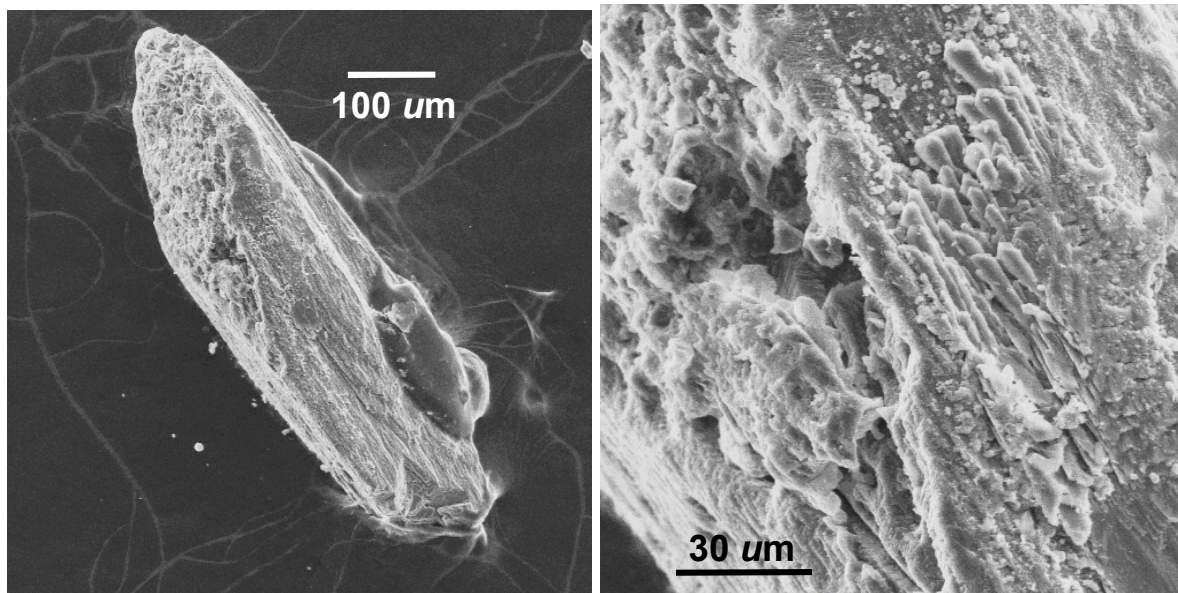


Figure 6. Secondary electron SEM micrograph of magnesite (figure on left) from the supercritical CO<sub>2</sub>-brine-rock experiment. Magnesite crystals are large, up to a few mm in length, and occur as individual grains and splays. Close-up view (figure on right) illustrates pitted crystal faces, indicative of disequilibrium and interpreted as dissolution of early-formed magnesite.

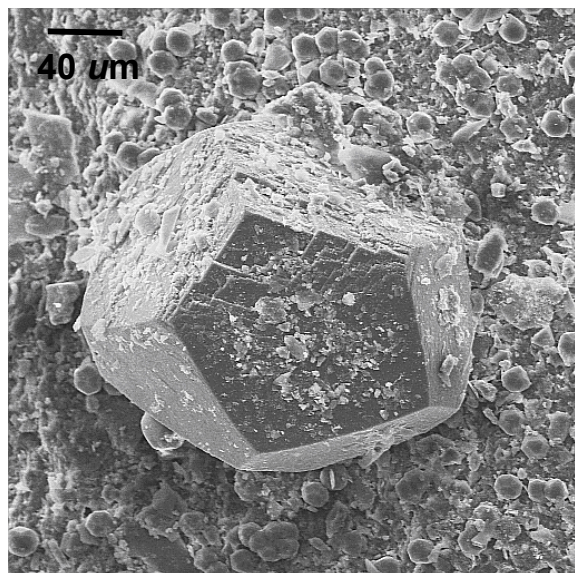


Figure 7. Secondary electron SEM micrograph of siderite from the supercritical CO<sub>2</sub>-brine-rock experiment. Siderite occurs as individual crystals, about 200-250 μm in diameter, growing on shale. Euhedral texture, indicative of equilibrium, is interpreted as precipitation of siderite after early-formed magnesite. Small, rounded grains surrounding the siderite are euhedral analcime.

experiment, ranging in size from 80 to 120 μm in diameter (Figure 9). Skeletal textures are interpreted as indicating acceleration of normal crystal nucleation and growth, possibly due to acidity in the brine or to the presence of an immiscible supercritical carbon dioxide phase.

## 4 DISCUSSION

### 4.1 Mixed Fluid Reactions and Processes

In agreement with models proposed for geologic sequestration of carbon (e.g., Gunter *et al.*, 2000), addition of supercritical carbon dioxide into the experimental brine-rock (aquifer plus aquitard) system decreased brine pH and precipitated carbonate minerals. The pressure decrease following injection of carbon dioxide indicates a decrease in the volume of the system due to the phase change of supercritical carbon dioxide, to dissolved carbonate, to mineral carbonate. In addition to pH decrease and carbonate mineral precipitation, a diversity of other fluid-rock reactions took place between the mixed fluid (immiscible supercritical carbon dioxide plus brine, Figure 1) and rock that differ from the brine-rock system.

Supercritical carbon dioxide supplied carbonate to buffer the fugacity of aqueous carbonate and hence

the pH of brine in the experimental system. The ability of an actual siliciclastic aquifer to buffer acidity and control geochemical reactions (*i.e.*, a rock-dominated system) may yield to acid-dominated and related reactions controlled by mixed fluid equilibria (*i.e.*, a fluid-dominated system). Adding to the complexity is the pH increase following pressure and temperature decrease and the accompanying loss of saturated carbon dioxide from acidic brine. For a brine-rock system into which supercritical carbon dioxide is catastrophically introduced, whether by anthropogenic injection from above or geologic emplacement from below, the sudden perturbation of on-going reactions may profoundly change the manner in which the geochemistry of the system ultimately evolves.

Acidified brine reacted with biotite and shale (Kaszuba *et al.*, 2003) to immediately enrich the brine in Mg (74x), Fe (188x), and Mn (5x) relative to the brine-rock system (Figure 4). Subsequent precipitation of carbonate mineral decreased concentrations of these elements in the brine, although the concentrations remained greater (Mg, 63x; Fe, 110x; and Mn, 3x) than in the brine-rock experiment. In contrast, reactions in the brine-rock experiment continued to add Mg, Fe, and Mn into solution as the rock reacted to equilibrate with NaCl brine. Without supercritical carbon dioxide and acidified brine, it is unknown whether concentrations of Mg, Fe, and Mn would converge in the two experiments. However, slight differences in minerals and assemblages exposed to the brine, could explain the divergence between experiments.

Sodium and potassium concentrations, as well as steady state chloride concentrations, decreased in acidified brine (Figures 2 and 5). Although sodium concentrations are also decreasing in the brine-rock experiment, and euhedral analcime precipitates in both systems, the rate of sodium decrease is approximately 10 times greater in the supercritical carbon dioxide-brine-rock experiment (Figure 10). Crystallization of analcime that is 2 to 6 times larger than early-formed analcime and exhibits skeletal texture presumably accounts for the rapid rate at which the concentration of sodium in the brine decreases. Whether large crystal size and skeletal texture is the result of accelerated growth in acidic brine or to the presence of immiscible supercritical carbon dioxide is not constrained by our experiments. However, it is clear that fluid-rock reaction rates are accelerated and analcime stability enhanced in an acidified brine-supercritical carbon dioxide system. The disposition of potassium is also not constrained by our experiments, although growth of clay minerals (smectite) on biotite and shale (Kaszuba *et al.*, 2003) may account for the decreased potassium



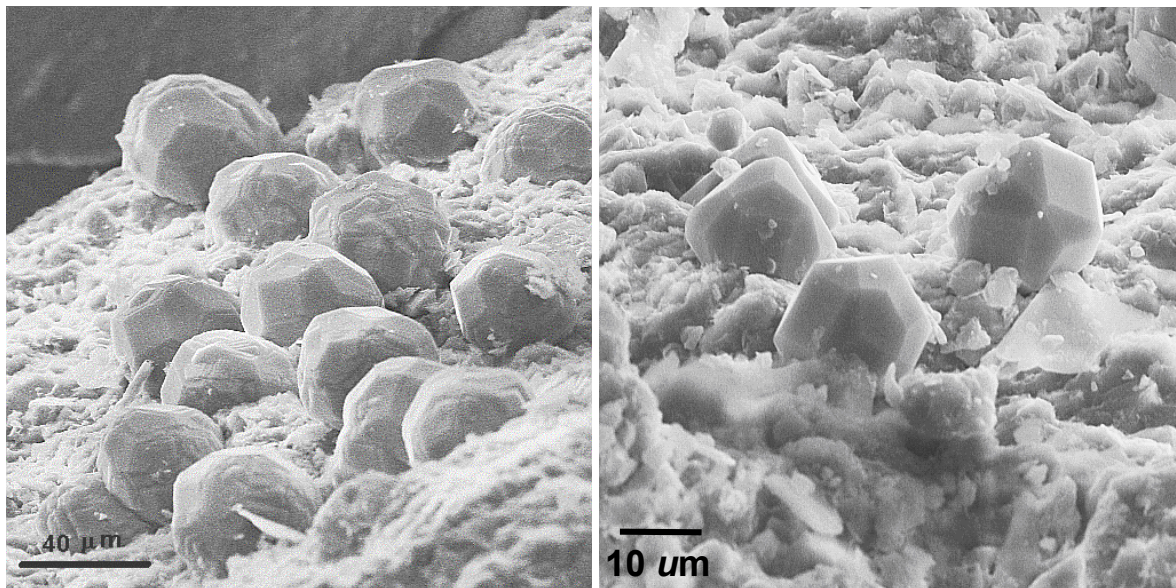


Figure 8. Secondary electron SEM micrograph of analcime on shale from experimental reaction of brine-rock (figure at left) and supercritical CO<sub>2</sub>-brine-rock (figure at right). Euhedral analcime crystals, 20-40 μm in diameter, occur on the shale and the aquifer minerals and are more abundant in the brine-rock experiment as compared to the supercritical CO<sub>2</sub>-brine-rock experiment. Euhedral textures are interpreted as equilibrium crystallization.

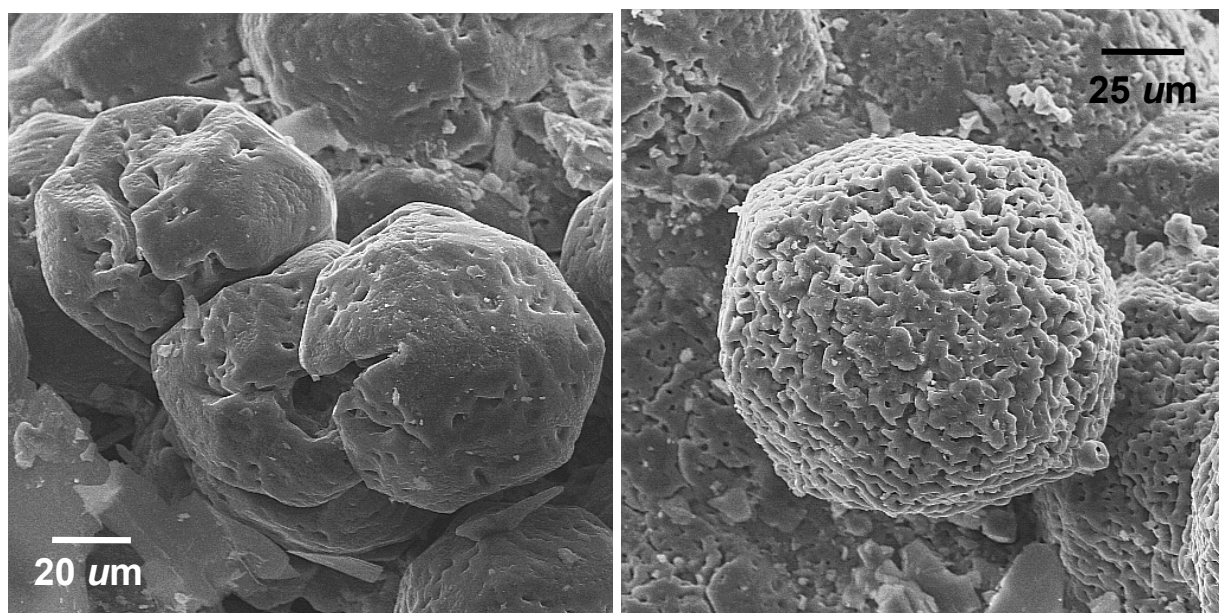


Figure 9. Secondary electron SEM micrograph of skeletal analcime from experimental reaction of supercritical CO<sub>2</sub>-brine-rock. Skeletal analcime crystals, ranging in size from 80 to 120 μm in diameter, occur in crystalline masses. Skeletal textures are interpreted to indicate accelerated crystal nucleation and growth, possibly due to acidity in the brine or to the presence of an immiscible supercritical CO<sub>2</sub> phase.

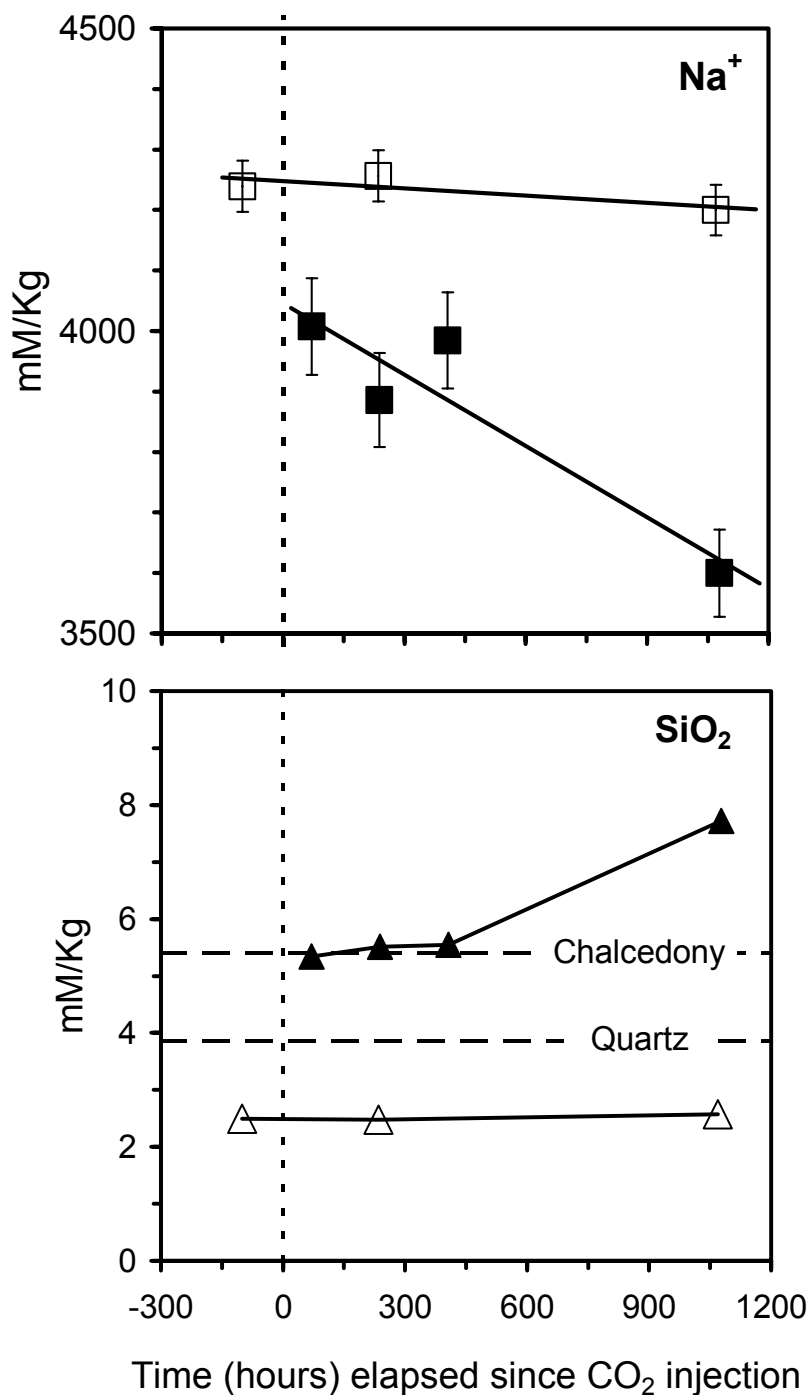


Figure 10. Relative rate of change of Na (top) and SiO<sub>2</sub> (bottom) concentration as a function of time elapsed since injection of CO<sub>2</sub> into reaction cell. Experimental reaction for brine-rock (open symbols) and supercritical CO<sub>2</sub>-brine-rock (solid symbols). Carbon dioxide was injected into the reaction cell of the supercritical CO<sub>2</sub>-brine-rock experiment at 0 hours (vertical dashed line). Compared to the brine-rock experiment, Na concentration in the supercritical CO<sub>2</sub>-brine-rock experiment decreases ~10x whereas SiO<sub>2</sub> concentration increases ~30x. Horizontal dashed lines are calculated solubility of chalcedony and quartz. Linear regression drawn through Na data whereas SiO<sub>2</sub> data are connected by line drawn between individual points. Uncertainties for Na analyses shown as error bars. Uncertainties for SiO<sub>2</sub> analyses are approximately the thickness of the line connecting the data points.

concentration. In the absence of chloride-bearing minerals (e.g. simple salts or chloride-bearing silicates such as scapolite), decreased chloride concentration may be due to exchange reactions with hydroxyls in the sheet silicates.

Silica concentrations are enhanced in the mixed-phase brine by a factor of two as compared to the brine-rock system, at a concentration comparable to the calculated solubility of chalcedony (Figure 10). And while both systems initially exhibit steady state silica concentrations followed by increasing silica concentration, the rate of increase is approximately 30 times greater in the supercritical carbon dioxide-acid brine system. Clearly, fluid-silicate reaction rates are accelerated and silica solubility is enhanced in an acidified brine-supercritical carbon dioxide system.

#### 4.2 Integrity of a Carbon Repository

In addition to dissolution of supercritical carbon dioxide into brine, pH decrease, and carbonate mineral precipitation, this study demonstrates that additional geochemical reactions and processes take place between the two-phase fluid (supercritical carbon dioxide and brine) and the aquitard as well as the aquifer minerals. These reactions may give rise to a number of geochemical and geotechnical consequences of significance to a carbon repository.

Increased acidity of the aqueous fluids within a carbon repository is a widely recognized and acknowledged consequence of carbon dioxide disposal (e.g., Gunter *et al.*, 2000). The potential for other reactions that may accompany migration of this fluid within the repository, however, has not been addressed. A pH increase accompanied the loss of saturated carbon dioxide from acidic brine within the experimental system (Figure 3). With movement of acidic brine to higher stratigraphic levels in a carbon repository, or leakage into overlying strata, water-rock reactions more characteristic of lower temperature, lower pressure, and neutral or even alkaline pH conditions become prevalent. Movement to distal regions of the repository that remain at pressure and temperature, yet away from the buffering influence of the supercritical carbon dioxide and related processes controlled by mixed fluid equilibria (i.e., a fluid-dominated system), may return the fluid to a system of rock-dominated reactions. As neutral pH conditions prevail, silica super-saturated brine may precipitate quartz, chalcedony, or amorphous silica. The same deleterious effects that result from carbonate mineral precipitation may also take place with silica mineral precipitation, including pore plugging and repository over-pressurization that encourage carbon dioxide leakage and loss of integrity.

Nucleation and growth of siderite on shale (Figure 7) as well as the minerals comprising the aquifer suggests the shale is a reactive component in the system. Shale reactivity may produce an increase in porosity and permeability, concomitant loss of system integrity, and subsequent release of carbon dioxide. Alternatively, reactivity of the shale may yield reaction products that fill porosity and decrease permeability, thereby enhancing the integrity of the repository. In either case, the impact of shale reactivity on the compressive and tensile strengths of the caprock, and hence the structural integrity of the repository, are currently unknown.

The occurrence of a paragenetic sequence of carbonate minerals (magnesite and siderite, Figures 6 and 7) indicates complexity of geochemical reactions among supercritical carbon dioxide, the in-place brine, the aquifer, and the aquitard. Precipitation of the mixed hydroxyl carbonate mineral dawsonite ( $\text{NaAlCO}_3(\text{OH})_2$ ), predicted as a stable carbonate phase in reactive transport models of carbon sequestration (Johnson *et al.*, 2002; Knauss *et al.*, 2002), was not observed in this study. In an effort to understand these complexities, we have calculated the saturation state of carbonate minerals in brine using data from Table 2. The results of these calculations (Figure 11) indicate that the brine is carbonate under-saturated in these experiments. Magnesite comes closest to achieving saturation, followed by siderite. The calculated mineral stability of siderite does not exceed magnesite. Clearly, the relevance of reaction path and reactive transport models that will be used to understand geochemical reaction within a carbon repository must be verified for consistency with experimental observation and evaluated for internal consistency with thermodynamic data. What unknown processes will these models not account for, and what will be the possible sources of error in applying these models?

Nucleation and accelerated mineral growth of skeletal analcime took place as a consequence of carbon dioxide injection, although the phenomenological cause of this process is not constrained by our experiments. Analcime, a mineral often attributed to zeolite facies metamorphic conditions, can crystallize in a repository at temperatures far below 200°C. Even without crystallization of analcime, the potential for changes to mineral nucleation and growth as a response to injection of carbon dioxide, and the resulting change in the mineral fabric of the host aquifer, have significant implication for a carbon repository. In addition to filling pores, enhanced growth of pre-existing or new minerals may increase the range of grain sizes present in the aquifer. This diminished quality of grain size sorting may reduce the

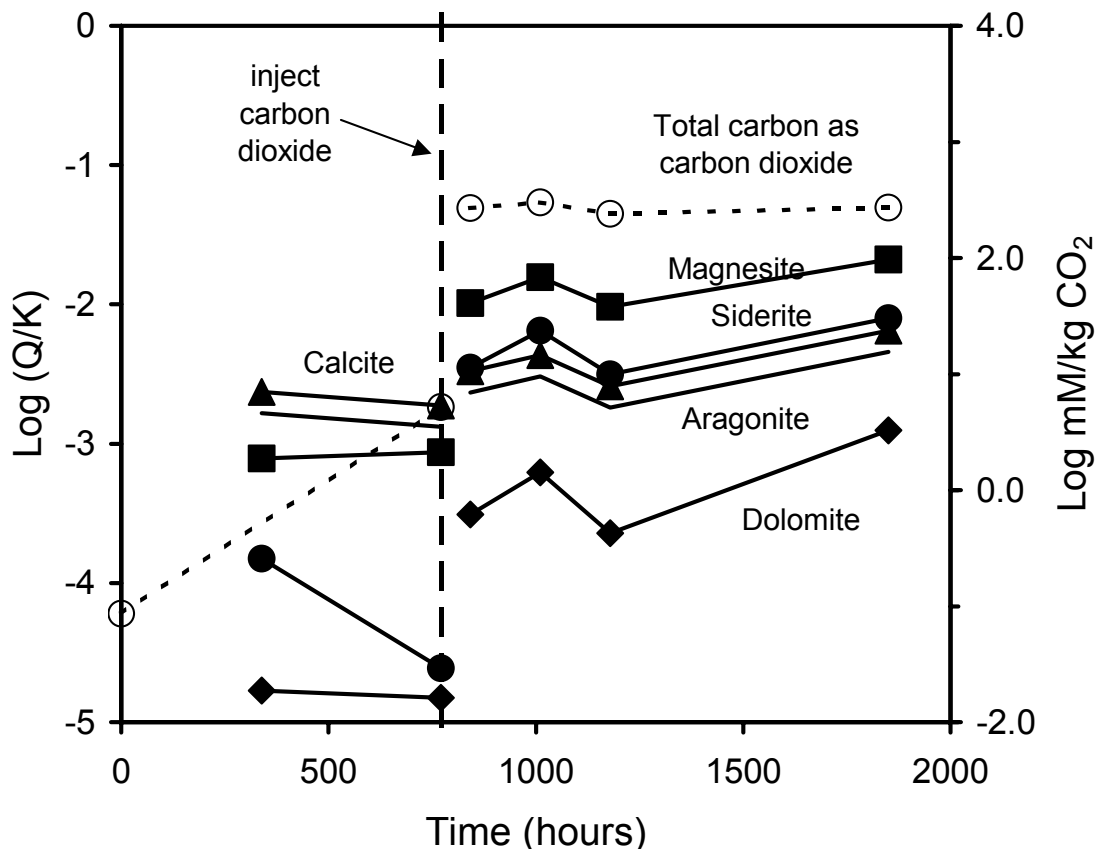


Figure 11. Calculated saturation state of magnesite (squares), siderite (circles), calcite (triangles), aragonite (no symbol used), and dolomite (diamonds) in supercritical CO<sub>2</sub>-brine-rock experiment. Calculations performed using Geochemist's Workbench, the resident database thermo.com.V8.R6+, and the b-dot ion association model (Bethke, 1998). Total carbon (as CO<sub>2</sub>) during the experimental reaction is plotted as open circles and dashed lines using the scale at the right.

permeability of the aquifer. Predicative computer models do not account for changes in mineral texture, or the resulting impact of these textural changes to fluid flow in a carbon repository.

Pressure increases accompanying injection of carbon dioxide are anticipated for a carbon repository, as mirrored in our experiments. Increased pressure has been suggested as a means of repository failure due to dilation of previously-sealed fractures and subsequent escape of carbon dioxide (Klusman, 2003). Plugging of pores due to precipitation of carbonate mineral may enhance the effect. Our work suggests that repository over-pressures from carbon dioxide injection may actually be somewhat alleviated by carbonate mineral precipitation but exacerbated by silica precipitation. In the dynamic reaction environment of a carbon repository, geochemically-induced pressure changes will affect the integrity of a carbon repository.

In addition to the large-scale influences on the integrity of a carbon reservoir, geochemical reactions

and processes identified in our experiments may provide important characteristics for monitoring and evaluation of repository performance. Silica supersaturation and increased alkalinity associated with mixed fluid phase equilibria could be monitored as geochemical indicators in interconnected or deep-seated aquifers, springs, or water wells. Changes in these chemical parameters may provide clues to the subsurface disposition of stored carbon dioxide and may also provide new perspectives for evaluating the dynamics of existing reservoirs containing supercritical carbon dioxide.

At a minimum, this experimental study demonstrates that mixed fluid reactions and related processes have potential for geochemical reactions that have not been sufficiently addressed in the carbon sequestration literature. Fracturing, loss of system integrity, and leakage of carbon dioxide may occur just as readily as self-healing of fractures. The beneficial (or deleterious) effects, and potential impacts to repository integrity, have yet to be

quantitatively identified. This rather elementary conclusion is consistent with the few studies that incorporate geochemistry into models of geologic sequestration (Gunter *et al.*, 2000; Gunter *et al.*, 1997; Perkins and Gunter, 1995) and adds a vast dimension of complexity and opportunity that must be understood if geologic sequestration in a carbon repository is to be successful.

#### 4.3 Implications for Silica Precipitation and Quartz Veins

In light of our experimental work, we suggest that multi-phase equilibrium relationships between supercritical carbon dioxide and brine-rock systems may be a source of silica cement in some sandstones and quartz mineralization in some veins. In the experimental system containing acidic brine and supercritical carbon dioxide, silica concentrations were enhanced by dissolution of silicate minerals and concomitant inhibition of the precipitation of quartz. In their evaluation of the mixing of hot hydrothermal solutions with ambient seawater at mid-ocean ridge vents, (Janecky and Seyfried, 1984) also noted silica super-saturation and inhibition of quartz precipitation. They attributed these phenomena to kinetics of silica polymerization and precipitation under acid pH conditions, assumptions consistent with recent experimental results (Icopini *et al.*, 2002). Return of a silica super-saturated brine into a rock-dominated reaction system buffered to more neutral pH conditions may enhance precipitation of quartz, chalcedony, or amorphous silica as veins or cements, depending on the structure of permeability.

## 5 CONCLUSIONS

This experimental investigation examines geochemical reactions and processes among supercritical carbon dioxide, brine, and host rock (aquifer and aquitard) simulating a carbon repository and evaluates fluid-rock reactions that may adversely impact the integrity of the repository. The following are concluded from these experiments:

1. Addition of supercritical carbon dioxide to a brine-rock system changes the system from rock- to fluid-dominated reactions.
2. A paragenetic sequence of carbonate mineralization (corroded magnesite and euhedral siderite) followed carbon dioxide injection. Nucleation and growth of siderite on shale suggests the aquitard is a reactive component in a carbon repository.
3. Precipitation of crystalline or amorphous silica from silica-supersaturated brine and pH increase may accompany migration of fluid within and from the repository. Enhancement in precipitation could armor and protect flow paths or plug them.
4. Accelerated mineral growth may change the fabric and permeability of the host aquifer, with the potential for adverse impact to a repository.
5. Besides direct application to geologic sequestration of carbon, an understanding of multi-phase fluid equilibrium relationships between supercritical carbon dioxide and aquifer-brine systems raises new questions and potential interpretations in a wide variety of natural geologic systems. In particular, multi-phase fluid equilibria may account for silica cement in some sedimentary basin sandstones and quartz vein mineralization in some ore districts.

#### Acknowledgements

Funding was provided by Los Alamos National Laboratory (LDRD/DR) for this research and by the US Department of Energy, Basic Energy Sciences, Geosciences Program for the hydrothermal laboratory facilities. Dale Counce provided brine analyses.

## REFERENCES

- Bachu, S., 2000. Sequestration of CO<sub>2</sub> in geological media: Criteria and approach for site selection in response to climate change. *Energy Conversion and Management*, 41(9): 953-970.
- Bachu, S., 2002. Sequestration of CO<sub>2</sub> in geological media in response to climate change: road map for site selection using the transform of the geological space into the CO<sub>2</sub> phase space. *Energy Conversion and Management*, 43(1): 87-102.
- Bachu, S., Gunter, W.D. and Perkins, E.H., 1994. Aquifer disposal of CO<sub>2</sub>: Hydrodynamic and mineral trapping. *Energy Conversion and Management*, 35(4): 269-279.
- Benson, S.M., 2000. Advances in geologic sequestration: Identifying and addressing key issues. *Geological Society of America, Abstracts with Programs*, 32(7): A200.
- Bethke C. R. (1998) *The Geochemist's Workbench Release 3.0: A users guide*. University of Illinois at Urbana-Champaign.
- Carter, L.S., Kelley, S.A., Blackwell, D.D. and Naeser, N.D., 1998. Heat flow and thermal history of the Anadarko basin, Oklahoma. *AAPG Bulletin*, 82(2): 291-316.
- Ennis-King, J. and Paterson, L., 2000. Reservoir engineering issues in the geological disposal of carbon dioxide. In: D.J. Williams, R.A. Durie, P. McMullan, C.A.J. Paulson and A.Y. Smith

- (Editors), 5th International Conference on Greenhouse Gas Control Technologies, Cairns, Australia, pp. 290-295.
- Gunter, W.D., Perkins, E.H. and Hutcheon, I., 2000. Aquifer disposal of acid gases: modelling of water-rock reactions for trapping of acid wastes. *Applied Geochemistry*, 15(8): 1085-1095.
- Gunter, W.D., Wiwchar, B. and Perkins, E.H., 1997. Aquifer disposal of CO<sub>2</sub>-rich greenhouse gases: Extension of the time scale of experiment for CO<sub>2</sub>-sequestering reactions by geochemical modelling. *Mineralogy and Petrology*, 59(1-2): 121-140.
- Hitchon, B., Gunter, W.D., Gentzis, T. and Bailey, R.T., 1999. Sedimentary basins and greenhouse gases: A serendipitous association. *Energy Conversion and Management*, 40(8): 825-843.
- Huffmann, E., 1977. Performance of a new automatic carbon dioxide coulometer. *Microchemical Journal*, 22(4): 567-573.
- Hurter, S.J. and Pollack, H.N., 1996. Terrestrial heat flow in the Parana Basin, southern Brazil. *Journal of Geophysical Research*, 101(B4): 8659-8671.
- Icopini, G., Brantley, S. and Heaney, P., 2002. Kinetics of silica nanocolloid formation from supersaturated solutions. *Geochimica et Cosmochimica Acta*, 66(15A): A351.
- Janecky, D. and Seyfried, W., 1984. Formation of massive sulfide deposits on oceanic ridge crests - Incremental reaction models for mixing between hydrothermal solutions and seawater. *Geochimica et Cosmochimica Acta*, 48(12): 2723-2738.
- Johnson, J.W., Steefel, C.I. and Knauss, K.G., 2002. Reactive transport modeling of geologic CO<sub>2</sub> sequestration. *Geological Society of America, Abstracts with Programs*, 34(6): 390.
- Kaszuba, J.P. and Janecky, D.R., 2000. Experimental hydration and carbonation reactions of MgO: A simple analog for subsurface carbon sequestration processes. *Geological Society of America, Abstracts with Programs*, 32(7): A202.
- Kaszuba, J.P., Janecky, D.R. and Snow, M.G., 2003. Carbon dioxide reaction processes in a model brine aquifer at 200°C and 200 bars: Implications for geologic sequestration of carbon. *Applied Geochemistry*, 18(7): 1065-1080.
- Klusman, R., 2003. Evaluation of leakage potential from a carbon dioxide EOR/sequestration project. *Energy Conversion and Management*, 44(12): 1921-1940.
- Knauss, K.G., Steefel, C.I., Johnson, J.W. and Boram, L.H., 2002. Impact of CO<sub>2</sub>, contaminant gas, aqueous fluid, and reservoir rock interactions on the geologic sequestration of CO<sub>2</sub>. *Geological Society of America, Abstracts with Programs*, 34(6): 306.
- Lindeberg, E., 1997. Escape of CO<sub>2</sub> from aquifers. *Energy Conversion and Management*, 38(SS): S235-S240.
- Oldenburg, C.M., Pruess, K. and Benson, S.M., 2001. Process modeling of CO<sub>2</sub> injection into natural gas reservoirs for carbon sequestration and enhanced gas recovery. *Energy & Fuels*, 15(2): 293-298.
- Perkins, E.H. and Gunter, W.D., 1995. Aquifer disposal of CO<sub>2</sub>-rich greenhouse gases: Modelling of water-rock reaction paths in a siliciclastic aquifer. In: Y.K. Kharaka and O.V. Chudakov (Editors), *Proceedings of the 8th International Symposium on Water-Rock Interaction*. A.A. Balkema, Vladivostok, Russia, pp. 895-898.
- Pruess, K. and Garcia, J., 2002. Multiphase flow dynamics during CO<sub>2</sub> disposal into saline aquifers. *Environmental Geology*, 42(2-3): 282-295.
- Rutqvist, J. and Tsang, C., 2002. A study of caprock hydromechanical changes associated with CO<sub>2</sub>-injection into a brine formation. *Environmental Geology*, 42(2-3): 296-305.
- Saripalli, P. and McGrail, P., 2002. Semi-analytical approaches to modeling deep well injection of CO<sub>2</sub> for geological sequestration. *Energy Conversion and Management*, 43(2): 185-198.
- Seyfried, W.E., Jr., Janecky, D.R. and Berndt, M.E., 1987. Rocking autoclaves for hydrothermal experiments, II. The flexible reaction-cell system. In: G.C. Ulmer and H.L. Barnes (Editors), *Hydrothermal Experimental Techniques*. John Wiley & Sons, New York, pp. 216-239.
- Span, R. and Wagner, W., 1996. A new equation of state for carbon dioxide covering the fluid region from the triple-point temperature to 1100 K at pressures up to 800 MPa. *Journal of Physical and Chemical Reference Data*, 25(6): 1509-1596.
- Takenouchi, S. and Kennedy, G.C., 1964. The binary system H<sub>2</sub>O-CO<sub>2</sub> at high temperatures and pressures. *American Journal of Science*, 262: 1055-1074.